Journal of Nuclear Materials 415 (2011) S74–S77

Contents lists available at ScienceDirect

Journal of Nuclear Materials

journal homepage: www.elsevier.com/locate/jnucmat

Modeling of macroscopic melt layer splashing during plasma instabilities

G. Miloshevsky *, A. Hassanein

School of Nuclear Engineering, Center for Materials under Extreme Environment, Purdue University, West Lafayette, IN 47907, USA

ARTICLE INFO

Article history:
Available online 3 September 2010

ABSTRACT

Damage of plasma-facing components in tokamaks due to various plasma instabilities remains one of the most important problems for successful operation. Macroscopic melt losses from divertor plates and nearby components into core plasma are significant material erosion lifetime and plasma contamination issues. The linear stability analysis and computational modeling are used to predict the onset and growth of surface waves on the plasma–liquid metal interface. The whole course of development, growth, and breakup of waves is modeled for the first time. The new physics mechanism involved in breakdown of a thin melt layer is presented. It is found that the melt layer undergoes macroscopic motion, bulk melt splitting, development and growth of liquid tungsten ligaments that transform to thin threads and eventually break into droplets. These results shed light on the physical behavior of a melt layer under transient plasma instabilities such as edge-localized modes and disruptions.

1. Introduction

Transient heat loads due to plasma disruptions (20–100 MJ/m^2) and edge-localized modes (ELMs, ~1–3 MJ/m^2) can erode divertor materials in tokamak devices [1]. The deposited high-heat power can generate vapor cloud, melt plasma-facing materials, causes ejection of droplets, with subsequent surface damage and serious plasma contamination [2]. One of the most significant problems during plasma instabilities is macroscopic melt losses from a metallic divertor plate and potential contamination of the core plasma. Melt layer splashing due to macroscopic melt motion was investigated in a number of laboratory experiments carried out using laser, electron and plasma accelerator devices with different heat loads and time durations [3]. The plasma impact momentum and/or Lorentz force were found to be responsible for melt splashing.

The behavior of the melt layer under plasma disruptions is not well understood. The development of Kelvin–Helmholtz (K–H) instability at the plasma–melt interface could be one of the mechanisms for the loss of a melt layer [4]. The high-speed plasma can produce surface melt perturbations and growth of waves. Breakup of surface waves can later result in liquid droplets formation and their ejection or splashing into the plasma.

The theoretical studies and modeling of momentum transfer from the impacting plasma or other volumetric forces (e.g., Lorentz force) to a melt layer are very important for understanding the physical mechanisms involved in splashing and droplet formation. The classical linear stability analysis and computer simulations were used to study the onset of instability, development and growth of surface waves, and formation of liquid tungsten droplets dragged by the plasma flow [5]. In this previous work, the continuous liquid tungsten ligaments, their elongation by the plasma flow and development of long, thin threads that eventually can break into liquid droplets were predicted. In the present work, the linear stability analysis is specifically adapted to the case of plasma and melt layers of different thicknesses used in the simulations. The melt behavior in a wide range of wavelengths is investigated. An intimate link between the predictions of the linear stability analysis and comprehensive computer simulations is illustrated. It is clearly shown that long and short waves are damped, but under considered plasma conditions intermediate waves (~2 mm) develop and grow rapidly disrupting the melt.

2. Theoretical and computational models

A linear analysis of the K–H instability [6] is applied to the flow of tungsten and plasma fluids of different densities ρ_m and ρ_p ($\rho_m \gg \rho_p$) and velocities V_m and V_p ($V_p \gg V_m$) flowing along the x direction in plane (x, y) with the lighter plasma above the liquid layer. The gravity $\mathbf{g}$ and the interfacial surface tension γ are taken into account. We adapted the linear stability analysis given in a textbook of Chandrasekhar [6] for inviscid and infinitely thick fluids to our plasma–liquid metal system with extension to account for finite thicknesses of melt layer, h_m, and plasma flow, h_p. The following dispersion relation was derived [7]

* Corresponding author. Address: Nuclear Engineering Building, 400 Central Drive, West Lafayette, IN 47907-2017, USA.
E-mail address: gennady@purdue.edu (G. Miloshevsky).

0022-3115/$ - see front matter © 2010 Elsevier B.V. All rights reserved.
doi:10.1016/j.jnucmat.2010.08.032

$$\omega = -k_x\left(\frac{\rho'_m V_m + \rho'_p V_p}{\rho'_m + \rho'_p}\right) \pm \sqrt{\left(\kappa g\frac{\rho_m - \rho_p}{\rho'_m + \rho'_p} + \frac{\kappa^3\gamma}{\rho'_m + \rho'_p}\right) - \frac{k_x^2\rho'_m\rho'_p}{(\rho'_m + \rho'_p)^2}(V_m - V_p)^2}, \quad (1)$$

where $\rho'_m = \rho_m \coth(\kappa h_m)$ and $\rho'_p = \rho_p \coth(\kappa h_p)$, $\kappa = \sqrt{k_x^2 + k_y^2} = 2\pi/\lambda$ is the real wave number associated with small interface disturbances proportional to $\exp(i(k_x x + k_y y + \omega t))$, k_x and k_y are the x and y components of the wave number vector $\boldsymbol{\kappa} = k_x\mathbf{i} + k_y\mathbf{j}$ with $\mathbf{i}$, $\mathbf{j}$, are the Cartesian unit vectors along the x and y axes, λ is the wavelength, and ω is the frequency. The function under the square root in Eq. (1) denoted here as F describes an interplay between the stabilizing forces of gravity and surface tension for long and short waves (first two terms in brackets) and the destabilizing force of inertia (third term).

When the inertial force overcomes the restoring forces of gravity and surface tension (the expression under the square root is negative), the K–H instability develops. The maximum (critical) velocity difference from Eq. (1) can be written as

$$\Delta V = |V_m - V_p| > \sqrt{\frac{\rho'_m + \rho'_p}{\rho'_m\rho'_p}\left(\frac{G}{\kappa} + \gamma\kappa\right)}, \quad (2)$$

where $G = g(\rho_m - \rho_p)$ is the gravitational restoring force, and we assumed that $k_x = \kappa$ in deriving Eq. (2).

A computational model treats the plasma–liquid metal flow as the two immiscible fluids of different densities separated by a sharp interface. The volume of fluid (VOF) method [8] is used to describe the two-fluid flow as a composition of two pure fluids with volume fractions of plasma α_p and liquid metal α_m near the interface ($\alpha_p + \alpha_m = 1$), where away from the interface the flow contains only one fluid. In the VOF approach, a single-field velocity and pressure are used for both liquid metal and plasma. The velocity field is assumed to be continuous at the interface, but the pressure undergoes a jump due to the surface tension. The liquid metal and plasma fluids are considered incompressible, since estimates of mass wave speeds show that they are much slower than sound speeds, thus justifying the assumption of incompressibility. As the density of plasma is a constant, a continuity equation for the volume fraction of the plasma is given by

$$\frac{\partial\alpha_p}{\partial t} + \nabla\cdot(\alpha_p\mathbf{V}) = 0, \quad (3)$$

where $\mathbf{V} = (V_x, V_z)^T$ is the single velocity field. The liquid metal volume fraction is then computed as $\alpha_m = 1 - \alpha_p$. The incompressible single momentum equation can be written as

$$\rho\frac{\partial\mathbf{V}}{\partial t} = -\nabla p + \mathbf{F}_\sigma + \rho\mathbf{g}, \quad (4)$$

where p is the single field pressure, ρ is the volume-fraction-averaged density that depends on the densities of each fluid as $\rho = \alpha_p\rho_p + \alpha_m\rho_m$. The vaporization of tungsten at the plasma–liquid interface is neglected, so the energy equation is not solved in this case. The surface tension effect is modeled by using the continuum surface force method [9]. This method transforms surface tension into an equivalent volumetric force. It can be expressed as $\mathbf{F}_\sigma = \sigma\zeta\rho\mathbf{n}/(0.5(\rho_p + \rho_m))$, where σ the surface tension coefficient, $\mathbf{n} = \nabla\alpha_p$ the surface normal defined as the gradient of α_p, and ζ the interfacial curvature. The Eqs. (3) and (4) are solved using the commercial FLUENT program package.

3. Analytical and computational results

The onset of instability is analytically analyzed using the classical linear stability theory [6,7]. For typical plasma disruptions, the plasma velocity is estimated to be in the range 10^6–10^7 cm/s as predicted by HEIGHTS simulation package [10]. The velocity of melt motion is on the order of 10^2 cm/s [4]. The density of the impacting plasma is $\rho_p \sim 10^{-10} - 10^{-9}$ g/cm^3. The parameters of tungsten melt: $\rho_m = 17.6$ g/cm^3, $\gamma = 2500$ dyn/cm and $h_m \leqslant 0.04$ cm. The gravity constant is $g = 981$ cm/s^2. The function F (solid curve) and maximum velocity difference ΔV (dashed and dotted curves) are shown in Fig. 1 for a tungsten melt layer with $h_m = 400$ μm. The negative values of F correspond to the range of unstable wavelengths. The most "dangerous", fastest growing wave corresponds to $\lambda \sim 2.2$ mm. The curves for F with $h_p = 1.6$ mm and $h_p \approx \infty$ were superimposable meaning that a plasma layer with $h_p = 1.6$ mm can be considered as infinitely thick. The maximum velocity curve ΔV is parabolic-like in the case of an infinitely thick plasma layer, $h_p \to \infty$. The critical wavelength λ_c corresponds to the minimum velocity difference required to produce the growing K–H waves. The waves with wavelengths larger than λ_c are damped due to gravity effects. The waves with wavelengths smaller than λ_c are suppressed due to surface tension effects. The unstable region is above this curve. The plasma with $h_p = 1.6$ mm can be used in the simulations to accurately describe the range of unstable wavelengths. However, the dashed and dotted curves are quite different for long wavelengths that are not of a practical interest as the length of the computational domain is limited to 10 mm (see Fig. 2). It is seen that the fastest growing waves with $\lambda \sim 2.2$ mm on the melt layer with $h_m = 400$ μm can be generated by the plasma stream with the velocity ~100 km/s.

We have simulated the flow of two incompressible, inviscid, and immiscible plasma–liquid tungsten fluids separated by a sharp interface under the effects of gravity and surface tension. A sketch of the 2D computational domain is shown in Fig. 2. The two-fluid flow zone is 10 mm long and 2 mm high. The domain's length of ~10 mm corresponds to the element's length in the tungsten macrobrush design [4]. The melt layer thickness is $h_m = 400$ μm. The mesh with 400 × 80 cells (step size 25 μm) was used. The periodic boundary conditions are applied in the flow direction. The top and bottom domain boundaries are modeled as frictionless walls. Volume fractions and densities of two fluids are implemented in the C code as a user defined function (UDF) and used within the FLUENT solver. To initiate the instability, an initial sinus perturbation of the two-fluid interface $\sim a\sin(2\pi\times\lambda)$ with amplitude a and wavelength λ was also coded as UDF. The amplitude of perturbation at the interface was within a computational cell. The plasma and

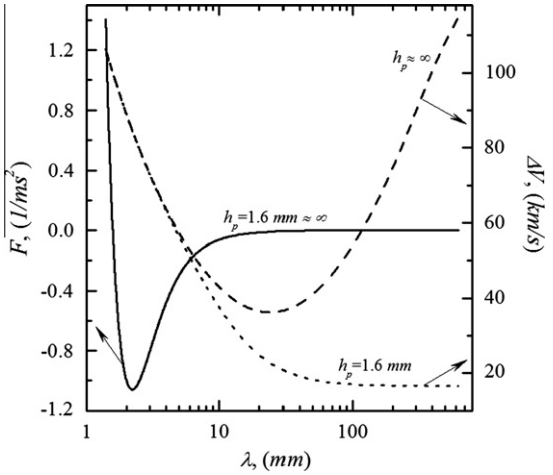

Fig. 1. Stability function (solid curve) and velocity difference (dashed and dotted curves) as a function of wavelength, $\lambda = 2\pi/\kappa$, for a tungsten melt layer with $h_m = 400$ μm. The arrows indicate the axis to which the curves belong. The density of impacting plasma is 10^{-9} g/cm^3.

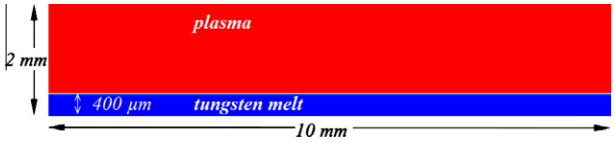

Fig. 2. Representative sketch of the computational domain used in simulations of two-fluid plasma–liquid tungsten flows. Liquid tungsten is shown in blue and plasma is displayed in red. (For interpretation of the references to colour in this figure legend, the reader is referred to the web version of this article.)

tungsten melt velocities are taken to be 10^7 cm/s and 10^2 cm/s, respectively. The plasma density is 10^{-9} g/cm^3. The nonlinear growth of waves was investigated for initial surface disturbances within the range from 1 to 50 wavelengths (λ = 0.2–10 mm). We present the results of simulations demonstrating the most interesting features of the breakdown mechanism of a melt tungsten layer.

Fig. 3 shows the temporal evolution of a small amplitude initial disturbance at the plasma–liquid metal interface with two wavelengths of λ = 5 mm. We can see that long waves do not grow as time increases. Melt is affected within a thin surface layer. The bulk of metallic melt is not disrupted during long times (~60 μs). Rupture of the tungsten melt into liquid droplets is also not observed. The same behavior was found for a wavelength with λ = 10 mm. These simulation results confirm the outcomes of the linear stability theory predicted that long wavelengths are stable (Fig. 1, solid curve).

The temporal behavior of the interface with an initial perturbation wavelength of λ = 2 mm (five wavelengths) is demonstrated in Fig. 4. The liquid tungsten waves grow quickly in amplitude at t = 0.48 μs. Small saw tooth-like secondary instability fingers are developed. At t = 1.45 μs, the plasma flow elongates further liquid metal waves forming five localized protrusions (ligaments). The width of ligaments is smaller than their lengths. As ligaments lengthen, they become curved and thinner. The ligaments collide capturing small pockets of the plasma (t = 4 μs). At t = 8 μs, the topological structures of liquid tungsten patterns suspended in the plasma become highly irregular. Melt layer losses are estimated to range from 80% to 90% of the initial melt thickness. There is a thin liquid tungsten film still remaining at the bottom.

The evolution of an initial disturbance at the plasma–liquid tungsten interface with 20 wavelengths (wavelength is λ = 0.5 mm) is shown in Fig. 5. The surface disturbances with this wavelength are stable according to the linear stability theory (Fig. 1). At t = 6.5 μs, the original wave crests are regularized by

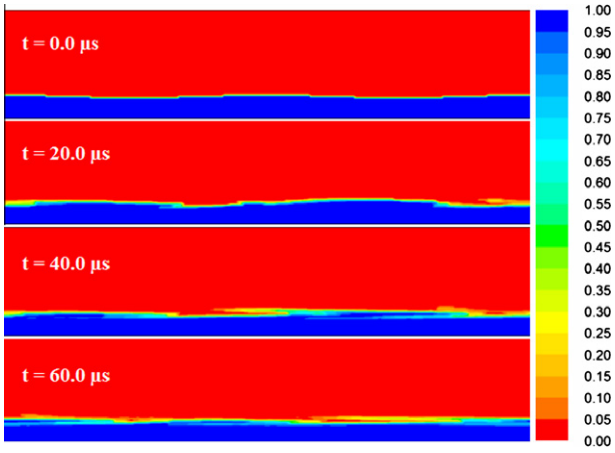

Fig. 3. Fields of volume fractions for plasma–liquid tungsten flow at different times. Two wavelengths with λ = 5 mm were initially excited at t = 0.0 μs.

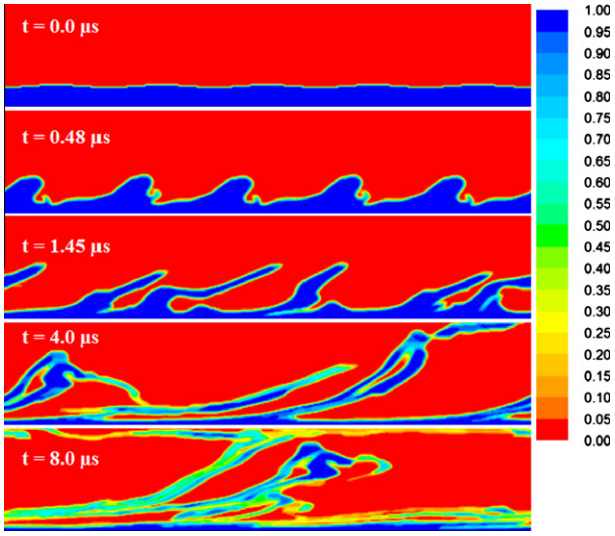

Fig. 4. Evolution in time of volume fraction fields for plasma–liquid tungsten flow. Five wavelengths with λ = 2 mm were initially excited at t = 0.0 μs.

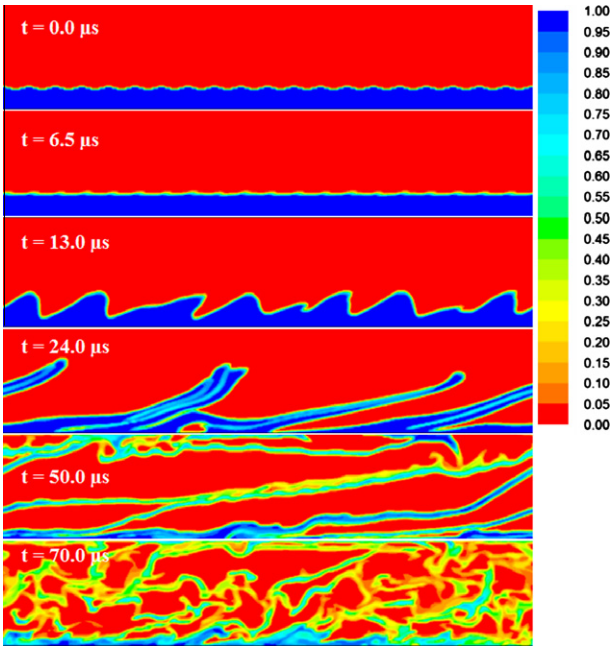

Fig. 5. Plasma–liquid tungsten volume fraction fields as a function of time. Twenty wavelengths with λ = 0.5 mm were initially excited at t = 0.0 μs.

the surface-tension force which strongly damps short waves (Fig. 1). Ripply wave structures without vortices induced by the plasma flow are seen (t = 6.5 μs). Thus, the interface is stable to disturbances with a wavelength of 0.5 mm in agreement with the linear analysis. However, the development and growth of new waves with larger wavelengths in agreement with predictions from the linear stability theory is observed at t > 10 μs. These most dangerous and fastest growing waves self-develop. Their wavelength is within 2 mm. The growth of melt waves splitting the bulk of the melt layer is seen at t = 13 μs. These liquid tungsten waves transform to elongated ligament protrusions penetrating into the plasma (t = 24 μs). An influx of tungsten from the bottom supports the ligament lengthening. Coalescence of ligaments occurs due to their collisions. During ligament agglomerations, bubbles of plasma become trapped and confined within a tungsten melt. Narrow

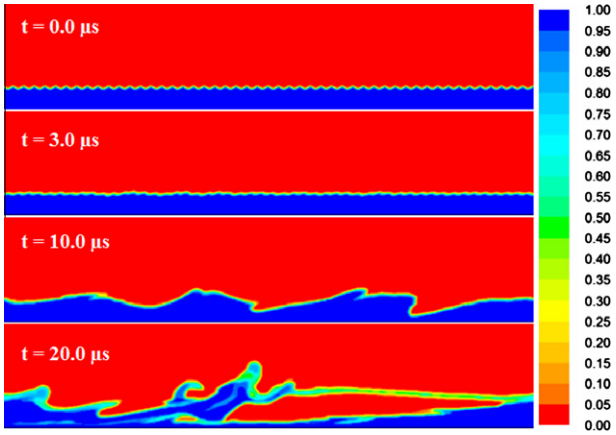

Fig. 6. Volume fraction fields of plasma–liquid tungsten flow at different times. Fifty wavelengths with $\lambda = 0.2$ mm were initially excited at $t = 0.0$ μs.

and long liquid tungsten threads are formed at $t = 50$ μs. The plasma flow changes the shape of threads creating thinner and thinner segments. This effect is due to sufficiently large surface-tension force of tungsten liquid holding the thread's interface together for long times. The thin threads are still bounded to the bottom ($t = 50$ μs). However, these liquid threads are highly thinned and eventually can break into droplets ($t = 70$ μs). Droplet size and number could be estimated from the diameter and length of ligaments. The estimates show that droplet sizes are within the range of ~25–200 μm.

Fig. 6 shows the time evolution of an initial wavy disturbance with a wavelength of $\lambda = 0.2$ mm (50 wavelengths). This test case was run until approximately 20 μs to verify if smaller wavelengths are severely suppressed by the surface-tension force with the plasma-melt system transiting from a short wavelength regime into a long wavelength mode as it is observed in the previous simulation. It is seen in Fig. 6 that these short wavelength corrugations are regularized faster (at $t = 3$ μs). At $t = 10$ μs, the four large waves develop and undergo localized growth with subsequent transformations into ligaments. Similarly, as in Fig. 4, the further behavior of ligaments is again irregular ($t = 20$ μs).

4. Summary

This work focuses on understanding the underlying physical processes involved in the breakdown and erosion mechanism of a liquid metal layer, macroscopic melt motion, and losses during plasma instabilities such as edge-localized modes and disruptions in tokamaks. Linear stability analysis and computer simulations of the entire process of development, growth, and breakup of waves at the plasma–liquid metal interface are presented for the first time. The inviscid stability analysis predicts that plasma streams with velocities of $\sim 10^7$ cm/s and densities $\sim 10^{-9}$ g/cm^3 can generate the growth of surface disturbances on a thin melt layer ($h_m \approx 400$ μm). Short-length waves are strongly damped by the surface-tension force. Long waves do not grow on the surface of a melt layer with the length of 10 mm and the depth of 400 μm. It is found analytically and numerically that under considered plasma conditions the most dangerous waves correspond to $\lambda \sim 2$ mm (five wavelengths). The surface disturbances with 20 and 50 wavelengths were initially regularized by the surface-tension force. However, these short wavelength disturbances give rise to the growing of new waves with a critical wavelength on the order of ~2 mm. These relatively long waves in comparison to the melt thickness (0.4 mm) undergo localized growth with transformations into long ligaments and threads that eventually can fragment into liquid droplets. It is predicted that due to the plasma impact about 80–90% of a melt layer can be lost in the form of macroscopic liquid ligaments. Because the adhesion force stabilizing liquid tungsten near the solid-melt interface was not included in the modeling, this fraction may be overestimated. Thus, the bulk of the melt layer initially splits and disintegrates into ligaments and further into liquid droplets. Recent experiments on melt splashing carried out in the TEXTOR device clearly demonstrated the loss of molten tungsten in the form of continuous fine spray with droplets [11]. This mechanism of melt layer losses is completely different from that assuming the K–H instability is induced by the "plasma wind" on the surface of a melt with droplets formed at peaks of surface waves and dragged away by the plasma flow [4], thus not affecting the depth of a melt layer. This classical picture of the K–H instability is not observed in our simulations. No surface waves which amplify to form a periodic array of compact spanwise rollers with conventional K–H finger-like projections that eventually break off to form droplets are revealed.

Acknowledgements

This work is supported by the US Department of Energy, Office of Fusion Energy Sciences. TeraGrid computational resources provided by the NCSA under Grant TG-PHY090096. The authors acknowledge the NCSA for providing FLUENT software.

References

[1] G. Federici, Phys. Scripta T124 (2006) 1.
[2] A. Hassanein, V. Belan, I. Konkashbaev, et al., J. Nucl. Mater. 241–243 (1997) 288.
[3] G. Federici, A. Zhitlukhin, N. Arkhipov, et al., J. Nucl. Mater. 337–339 (2005) 684.
[4] B. Bazylev, G. Janeschitz, I. Landman, et al., Phys. Scripta T128 (2007) 229.
[5] G. Miloshevsky, A. Hassanein, Nucl. Fusion, submitted for publication.
[6] S. Chandrasekhar, Hydrodynamic and Hydromagnetic Stability, Oxford University, London, 1961.
[7] M. Ishii, T. Hibiki, Thermo-fluid Dynamics of Two-Phase Flow, Springer, Purdue University, 2006.
[8] C.W. Hirt, B.D. Nichols, J. Comput. Phys. 39 (1981) 201.
[9] J.U. Brackbill, D.B. Kothe, C. Zemach, J. Comput. Phys. 100 (1992) 335.
[10] A. Hassanein, I. Konkashbaev, J. Nucl. Mater. 273 (1999) 326.
[11] J. W. Coenen, B. Bazylev, S. Brezinsek, et al., J. Nucl. Mater. 2010, submitted for publication.